

NASA Technical Memorandum 107072

# Static Flow Characteristics of a Mass Flow Injecting Valve

Duane Mattern  
*NYMA Inc.*  
*Brook Park, Ohio*

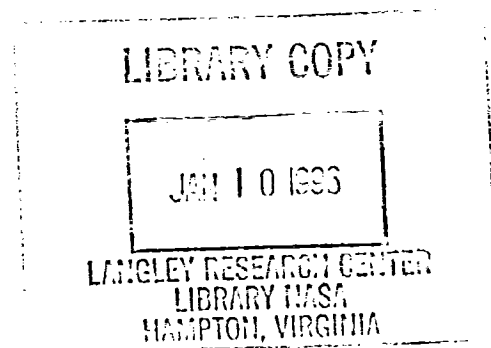
and

Dan Paxson  
*Lewis Research Center*  
*Cleveland, Ohio*

November 1995



National Aeronautics and  
Space Administration





## Static Flow Characteristics of a Mass Flow Injecting Valve

Duane Mattern  
NYMA, Inc.  
NASA Lewis Group  
Brookpark, OH 44142 USA  
(mattern@lerc.nasa.gov)

Dan Paxson  
Systems Dynamics Branch  
NASA Lewis Research Center  
Cleveland, OH 44135 USA  
(dpaxson@lerc.nasa.gov)

### Abstract

A sleeve valve is under development for ground-based forced response testing of air compression systems. This valve will be used to inject air and to impart momentum to the flow inside the first stage of a multi-stage compressor. The valve was designed to deliver a maximum mass flow of 0.22 lbm/s (0.1 kg/s) with a maximum valve throat area of 0.12 in<sup>2</sup> (80 mm<sup>2</sup>), a 100 psid (689 KPA) pressure difference across the valve and a 68°F, (20°C) air supply. It was assumed that the valve mass flow rate would be proportional to the valve orifice area. A static flow calibration revealed a nonlinear valve orifice area to mass flow relationship which limits the maximum flow rate that the valve can deliver. This nonlinearity was found to be caused by multiple choking points in the flow path. A simple model was used to explain this nonlinearity and the model was compared to the static flow calibration data. Only steady flow data is presented here. In this report, the static flow characteristics of a proportionally controlled sleeve valve are modelled and validated against experimental data.

### Introduction

Compression systems for jet engines have long been vexed by a region of flow uncertainty as shown on a typical compressor map in Figure 1. To gain an understanding of the fluid dynamics in this region of the compressor map, different models have been developed. These models need to be validated against experimental data to gain confidence in the predictions made by these computer codes. An experimental study of the fluid dynamics in a compression system requires a means by which to perturb the flow. In low speed compressors, (those with a rotational speed of less than about 6000 rpm) variable inlet guide vanes, bleed ports, the exhaust nozzle, and fuel flow have been used to excite the system. These actuation methods have bandwidths which are insufficient to excite some of the faster dynamics in high speed compression systems, (those with a rotational speed greater than about 6000 rpm). For example it has been shown that rotating stall fluid dynamics can have rotational speeds of 20-50 percent of the compressor shaft speed [1]. In order to excite the first three modes in a circumferential modal model of rotating stall [1], a bandwidth of 3 times the rotating stall speed would be required. For example, a compressor with a design speed of 18000 rpm, (300 rps), and a rotating stall at 50 percent of the shaft speed, an actuator with a minimum bandwidth of 450 Hz would be required to stimulate the first 3 modes represented by a modal model. Thus, the development of a high speed valve for injecting air into the first stage of a multi-stage compression system was undertaken to provide the enabling technology for compressor research.

A high speed prototype valve has been developed under the assumption that the valve exit air mass flow would be proportional to a variable choking orifice area within the valve. Static calibration of the prototype valve uncovered a nonlinear relationship between the valve orifice area and the exit mass flow, caused by multiple choking points in the flow. A simple static flow model of the valve was developed to understand the causes of this nonlinearity. In the following report, the static flow model is presented and the results predicted by this model are compared to the valve flow static calibration data.

### Valve Static Flow Model

Figure 2 is a schematic diagram of the prototype valve, with a cutaway section to reveal the valve interior and the flow path. Air enters the manifold through the supply line inlet area,  $A_0$ .  $A_0$  is sized so that the air manifold pressure is maintain near the supply line pressure. The air then passes through the controlled orifice area,  $A_1$ .  $A_1$  is proportional to the linear position of a sliding sleeve that cover a set of ports in the "arm" of the "sleeve" valve, as shown pictorially in Figure 3. The sleeve motion has a range of  $\pm 1$  millimeter. Once the air passes through  $A_1$ , it continues through a nearly constant area tube to the ejector exit area  $A_2$ . The important item to note in Figure 2 is the relative size of flow areas  $A_1$  and  $A_2$ . The points of interest in the flow are: "1", which denotes the upstream supply conditions; "2", which denotes the lumped volume between the supply and the sink (exit); and "3", which denotes the downstream exit conditions. Figure 4 shows a schematic diagram of the valve model geometry with points "1", "2", and "3" indicated. The following assumptions are made:

- 1)  $A_0$  is large enough to provide suffice mass flow to the largest orifice area,  $A_1$ .
- 2) The kinetic energy of the flow is lost after passing through the orifice area,  $A_1$ .
- 3) The system is adiabatic, (no heat exchange) and isentropic.
- 4) The working fluid, air, is calorically perfect, (ideal gas with constant specific heats).
- 5) No reverse flow will be encountered.

In Figure 4,  $T$ ,  $P$ ,  $\rho$ , and  $w$  indicate the temperature, pressure, density, and mass flow rate respectively. The mathematical model of the valve depicted in Figure 4 is relatively simple and is shown in Figure 5 as a block diagram. The calculation of the mass flow through  $A_1$ , ( $w_1$ ), and the mass flow through  $A_2$ , ( $w_2$ ), are represented by two of the blocks in Figure 5. The third block equalizes the mass flow through  $A_1$  and  $A_2$  using continuity and the energy equation. The mass flow calculations for area  $A_1$  are:

$$\text{PRF}_1 = \left[ \left( \frac{P_2}{P_1} \right)^{\frac{2}{\gamma}} - \left( \frac{P_2}{P_1} \right)^{\frac{1+\gamma}{\gamma}} \right]^{\frac{1}{2}} \quad (1)$$

$$w_1 = A_1 P_1 \left( \frac{g_c}{RT_1} \right)^{\frac{1}{2}} \left( \frac{2\gamma}{(\gamma-1)} \right)^{\frac{1}{2}} * \text{PRF}_1 \quad (2)$$

with

$\text{PRF}_1$  = Pressure Ratio Function (nondimensional)

- $w_1$  = mass flow through orifice  $A_1$ , (lbm/sec)  
 $A_1$  = orifice area, (ft<sup>2</sup>)  
 $P_1$  = upstream supply pressure, (psfg)  
 $T_1$  = upstream supply temperature, (deg R)  
 $P_2$  = pressure downstream of orifice, (psfg)  
 $R$  = ideal gas constant for air = 53.3 lb<sub>f</sub> f / (lbm deg R)  
 $g_c$  = English units conversion constant = 32.17 lb<sub>f</sub> f / (lbm s<sup>2</sup>)  
 $\gamma$  = specific heat ratio for air = 1.4

Equation (1) and (2) originate from reference [2] and are derived in the Appendix. In the mass flow rate calculation, the pressure ratio  $P_2/P_1$  is first checked for choked flow conditions. If the flow is not choked then the actual pressure ratio across the orifice is used in equation (1). If the flow is choked, then the choked flow pressure ratio, equal to 0.5282, is used. Note that the mass flow calculation is idealized and no discharge coefficient is assumed. Using equations (1) and (2) with the appropriate substitution of "3" for "2" and "2" for "1" yields the mass flow rate equations for area  $A_2$ :

$$\text{PRF}_2 = \left[ \left( \frac{P_3}{P_2} \right)^{\frac{1}{\gamma}} - \left( \frac{P_3}{P_2} \right)^{\frac{1+\gamma}{\gamma}} \right]^{\frac{1}{2}} \quad (3)$$

$$w_2 = A_2 P_2 \left( \frac{g_c}{RT_2} \right)^{\frac{1}{2}} \left( \frac{2\gamma}{(\gamma-1)} \right) * \text{PRF}_2 \quad (4)$$

The steady mass flow through  $A_1$  and  $A_2$  is balanced by varying the conditions in the lumped volume, "2" and recalculating the two mass flows until equalization is obtained. This is achieved by using a lumped volume at point "2" and allowing continuity and the energy equation to provide balancing of the mass flow rates. Continuity at point "2" yields:

$$\frac{d\rho_2}{dt} = \frac{(w_1 - w_2)}{V_2} \quad (5)$$

where

- $d\rho_2/dt$  = the time rate of change of the air density in the lumped volume, (lbm/ft<sup>3</sup>)  
 $V$  = the volume of the lumped system, (ft<sup>3</sup>)

An energy balance of the lumped volume yields:

$$\frac{dP_2}{dt} = \gamma R [ T_1 w_1 - T_2 w_2 ] \quad (6)$$

where  $T_1$  and  $T_2$  are total temperatures and  $c_p$  is the specific heat at constant pressure. Equations (5) and (6) are derived in the Appendix. Since  $T_1$  and  $T_2$  are total temperatures, and there is no heat addition, then  $T_2=T_1$ . It can be observed from equations (5) and (6) that steady flow requires  $w_1=w_2$ . Eqs. (5) and (6) represent simplified volume dynamics for section "2". Currently, these equations are only used to balance the mass flows for this static valve model.

## Derivation of Nonlinear Flow Relationship

During the design of this prototype valve, it was assumed that there would be one choking point in the flow, that this point would be at the controlled valve orifice area, point "1", and that it would always be choked for sufficient supply pressures. For choked flow and a fixed supply pressure,  $PRF_1$  from equation (1) would then be a constant, ( $P_2/P_1=0.5282$  for choked flow). Plugging this constant  $PRF_1$  into equation (2) yields an equation for the mass flow rate,  $w_1$  that is only a function of controlled orifice area,  $A_1$  and this function is linear for constant values of  $P_1, T_1$ , and  $P_2$ . As it turns out,  $P_2$  is not constant. Under certain conditions, the flow can choke at point "2" and unchoke at point "1". Once the flow has unchoked at point "1",  $PRF_1$  is no longer constant and  $w_1$  becomes a function of  $A_1$  and a nonlinear function of  $P_2$ . The resulting nonlinear relationship can be shown in a nondimensional format by manipulating equations (1)-(4). During steady flow,  $w_1=w_2$  and equation (1) can be equated to equation (3) as shown below:

$$w_1 = w_2$$

$$A_1 P_1 \left( \frac{g_c}{RT_1} \right)^{\frac{1}{2}} \left( \frac{2\gamma}{(\gamma-1)} \right) PRF_1 = A_2 P_2 \left( \frac{g_c}{RT_2} \right)^{\frac{1}{2}} \left( \frac{2\gamma}{(\gamma-1)} \right) PRF_2 \quad (7)$$

The upstream supply conditions,  $P_1, T_1$ , and downstream sink condition,  $P_3, T_3$ , and exit area,  $A_2$ , are all known. The orifice area  $A_1$  is the only variable to manipulate and the lumped volume conditions,  $P_2, T_2$ , and  $\rho_2$  are the only unknowns. Noting that  $T_2=T_1$  as previously stated and cancelling like terms results in the following:

$$A_1 P_1 PRF_1 = A_2 P_2 PRF_2$$

$$A_1 P_1 \left[ \left( \frac{P_2}{P_1} \right)^{\frac{2}{\gamma}} - \left( \frac{P_2}{P_1} \right)^{\frac{1+\gamma}{\gamma}} \right]^{\frac{1}{2}} = A_2 P_2 \left[ \left( \frac{P_3}{P_2} \right)^{\frac{3}{\gamma}} - \left( \frac{P_3}{P_2} \right)^{\frac{1+\gamma}{\gamma}} \right]^{\frac{1}{2}} \quad (8)$$

Dividing through by the fixed, nonzero values  $A_2$  and  $P_1$  yields the following nondimensional mass flow function:

$$MFF = \frac{A_1}{A_2} \left[ \left( \frac{P_2}{P_1} \right)^{\frac{2}{\gamma}} - \left( \frac{P_2}{P_1} \right)^{\frac{1+\gamma}{\gamma}} \right]^{\frac{1}{2}} = \frac{P_2}{P_1} \left[ \left( \frac{P_3}{P_2} \right)^{\frac{3}{\gamma}} - \left( \frac{P_3}{P_2} \right)^{\frac{1+\gamma}{\gamma}} \right]^{\frac{1}{2}} \quad (9)$$

This mass flow function can be used to examine the static flow trends as a function of the area ratio, for fixed  $P_1, T_1, P_3$ , and  $A_2$ , without regard to units. The model was run to steady flow state for several different controlled orifice areas,  $A_1$ , for fixed values of  $P_1, T_1, P_3$ , and  $A_2$ . Figure 6 is a plot of the mass flow function, MFF, defined in equation (9), versus the area ratio,  $A_1/A_2$ , with  $P_1=100$  and  $P_3=14.7$  psig,  $T_1=68$  deg F, and  $A_1=0.07$  square inches). Also

plotted in Figure 6 are logical indications corresponding to choked flow for orifices  $A_1$  and  $A_2$ . For instances, in Figure 6, with an area ratio of 0.4,  $MFF=0.03$  and both  $A_1$  and  $A_2$  are choked and for  $A_1/A_2=0.8$ ,  $A_2$  is choked and  $A_1$  is unchoked. The choking at  $A_2$  causes  $P_2$  to be larger than  $P_3$ . A varying  $P_2$  and equations (1) and (3) lead to the nonlinear relationship from  $A_1$  to mass flow.

### Comparison to Experimental Data

The valve was calibrated in the Flow Calibration Lab at NASA Lewis Research Center. The mass flow was measured using a calibrated orifice upstream of the valve at several different supply pressures. Figure 7 is a schematic diagram of the flow calibration setup. The supply pressure was measured just upstream of the valve inlet area  $A_0$ . The mass flow was measured with the valve in its full closed position to get a bypass or leakage mass flow rate. This leakage mass flow was used to estimate a leakage flow area in order to properly compare the calibration data to the model generated data which does not include a leakage model. When the valve is fully closed, it is assumed that  $P_2=P_3$  and equation (2) is used to estimate a leakage area,  $A_{1\_leak}$ .  $A_{1\_leak}$  and  $w_{1\_leak}$  are used as the origin for the model estimated data. Thus the model area ratio and the model predicted mass flow are offset by  $A_{1\_leak}$  and  $w_{1\_leak}$  respectively. Figure 8 compares the actual flow calibration data to the model predicted data for supply pressures of 40, 60, and 80 psig, with atmospheric exit conditions and a fixed exit area of 0.07 inches<sup>2</sup>, (diameter = 0.3 inches). The model predicted mass flows do not match perfectly because the model is idealized, but the nonlinear trend observed in the data is represented by the model. It is clear that in order to maintain a single choking point at  $A_1$  over the entire range of operation of  $A_1$ , that the exit area  $A_2$  must be properly sized relative to the largest controlled orifice area,  $A_1$ , if linearity is to be maintained. Figure 9 is a plot of the mass flow to orifice area for the prototype valve with three different exit diameters, ( 0.3, 0.344, 0.375 inches), at one supply pressure, 100 psig. Note that the maximum possible mass flow increases with the increase in the exit diameter and the linear range of the valve operation is extended.

A linear function for orifice area to exit mass flow makes the valve easier to implement. Also, the increase in useable range allows the valve to deliver more mass flow, increasing the effectiveness of the valve for perturbing the fluid dynamics in a compressor. While only the static flow properties of the valve are being discussed here, it is important to note that to achieve this increase in mass flow an increase in the stroke of the sleeve is required. This will reduce the achievable bandwidth of the valve, for a fixed orifice geometry. The orifice geometry can be modified to obtain this increase mass flow range without changing the sleeve stroke if necessary to maintain the valve design bandwidth.

## Summary

A static flow model is used to predict the characteristics of a prototype air valve. The model predicted static mass flow as a function of controlled orifice area compare favorably with the prototype valve static calibration data. The nonlinear relationship between controlled orifice area and valve mass flow is properly represented by the static flow model. The model can be used to properly size the valve exit area to provide for a linear relationship between the controlled orifice area and the valve mass flow. This linear relationship also results in a larger maximum mass flow rate capability of the valve.

## Acknowledgements

The authors would like to thank J.D. St. Clair and Andrea Clary in the NASA Flow Calibration lab for providing the flow calibration of the prototype valve.

## References

- 1) Garnier V.H., Epstein A.H., Greitzer E.M., "Rotating Waves as a Stall Inception Indication in Axial Compressors", Journal of Turbomachinery, April 1991, Vol. 113.
- 2) Paxson Daniel E., "A Model for the Space Shuttle Main Engine High Pressure Oxidizer Turbopump Shaft Seal System", NASA TM 103697, Nov., 1990.
- 3) Fox R.W., McDonald A.T., Introduction to Fluid Mechanics, John Wiley & Sons, 1978, ISBN 0-471-01909-7, p x.

## Appendix

Derivation of Equations (1) and (2): The following analysis of seal leakage flow was original done for reference [2] and is applicable here. The flow consists of two sections, a nozzle region and a constant area duct region. Assume that the flow is isentropic and adiabatic. Continuity yields:

$$\begin{aligned} w &= \rho A u \\ w &= \frac{\rho}{\rho_o} \rho_o A M a \end{aligned} \tag{A1}$$

where

- w = mass flow rate through the nozzle, (lbm/s),
- $\rho$  = density of the gas at the nozzle, (lbm/f<sup>3</sup>),
- $\rho_o$  = density of the gas upstream of the nozzle, (lbm/f<sup>3</sup>)<sub>m</sub>
- ( )<sub>o</sub> = denotes upstream conditions,
- A = duct area, (sq. ft),
- u = gas velocity, (fps),
- M = gas Mach number, (nondimensional),
- a = sqrt(  $\gamma RTg_c$  ) = speed of sound at the nozzle, (fps),
- $\gamma$  = specific heat ratio, (nondimensional),
- R = ideal gas constant (lb<sub>f</sub> f / lbm deg R),
- T = local gas temperature, (deg R),
- $g_c$  = English units conversion constant = 32.17 lb<sub>f</sub> f / (lbm s<sup>2</sup>).

For a calorically perfect gas (isentropic):

$$\frac{P}{P_o} = \left( \frac{\rho}{\rho_o} \right)^\gamma = \left( \frac{T}{T_o} \right)^{\frac{\gamma}{\gamma-1}} \tag{A2}$$

Substituting for "a" in equation (A1), and using equation (A2) to replace "T" and  $\rho/\rho_o$  yields:

$$\begin{aligned} w &= \left( \frac{P}{P_o} \right)^{\frac{1}{\gamma}} \rho_o A M \sqrt{\gamma RT} \\ w &= \left( \frac{P}{P_o} \right)^{\frac{1}{\gamma}} \rho_o A M \sqrt{\gamma RT_o} \left( \frac{P}{P_o} \right)^{\frac{\gamma-1}{2\gamma}} \end{aligned} \tag{A3}$$

Using the definition of "total" enthalpy yields an equation for the square of the velocity:  
Noting that  $u^2=(Ma)^2$  and using equation (A4) yields:

$$\begin{aligned}
h_o &= h + \frac{u^2}{2} \\
c_p T_o &= c_p T + \frac{u^2}{2} \\
u^2 &= 2c_p(T_o - T)
\end{aligned} \tag{A4}$$

$$\begin{aligned}
a^2 M^2 &= 2c_p(T_o - T) \\
M^2 &= \frac{2c_p(T_o - T)}{\gamma R T} \\
M^2 &= \frac{2}{\gamma - 1} \left( \frac{T_o}{T} - 1 \right), \quad \text{using } c_p = \frac{\gamma R}{\gamma - 1} \\
M^2 &= \frac{2}{\gamma - 1} \left[ \left( \frac{P}{P_o} \right)^{\frac{1-\gamma}{\gamma}} - 1 \right], \quad \text{using } \frac{P}{P_o} = \left( \frac{T}{T_o} \right)^{\frac{\gamma}{\gamma-1}}
\end{aligned} \tag{A5}$$

Equation (A3) can be simplified using (A5) and the ideal gas law, ( $\rho_o = P_o/RT_o$ ), yielding:

$$\begin{aligned}
w &= \left( \frac{P}{P_o} \right)^{\frac{1}{\gamma}} A \frac{P_o g_c}{\sqrt{RT_o g_c}} \sqrt{\frac{2\gamma}{\gamma-1} \left[ \left( \frac{P}{P_o} \right)^{\frac{\gamma-1}{\gamma}} \left[ \left( \frac{P}{P_o} \right)^{-\frac{(\gamma-1)}{\gamma}} - 1 \right] \right]^{\frac{1}{2}}} \\
w &= A P_o \sqrt{\frac{g_c}{RT_o}} \left( \frac{2\gamma}{\gamma-1} \right)^{\frac{1}{2}} \left[ 1 - \left( \frac{P}{P_o} \right)^{\frac{\gamma-1}{\gamma}} \right]^{\frac{1}{2}} \left( \frac{P}{P_o} \right)^{\frac{1}{\gamma}} \\
w &= A P_o \sqrt{\frac{g_c}{RT_o}} \left( \frac{2\gamma}{\gamma-1} \right)^{\frac{1}{2}} \sqrt{\left[ \left( \frac{P}{P_o} \right)^{\frac{2}{\gamma}} - \left( \frac{P}{P_o} \right)^{\frac{1+\gamma}{\gamma}} \right]}
\end{aligned} \tag{A6}$$

which is the same as equations (1) and (2) in the body of this report.

Derivation of equation (5): This is simply the conservation of mass for a fixed control volume. M is the total mass in the lumped volume and V is the fixed volume.

Derivation of equation (6): Performing an energy balance on the control volume shown in Figure 4, using reference [3] and assuming no heat transfer and no work done on the control volume results in the following equation:

$$\begin{aligned}\frac{d}{dt}(M) &= w_{in} - w_{out} \\ \frac{d}{dt}(\rho V) &= w_{in} - w_{out} \\ \dot{\rho} &= \frac{w_{in} - w_{out}}{V}\end{aligned}\tag{A7}$$

$$0 = \frac{\partial}{\partial t} \int_{cv} e \rho dv + \int_{cs} (u + pv + \frac{v^2}{2} + gz) \rho u dA\tag{A8}$$

where

cv = control volume

cs = control surface

e = u + V<sup>2</sup>/2 + gz, total energy per unit mass

u = internal energy per mass

Substituting for "e" and assuming the potential terms gz are small yields:

$$\frac{\partial}{\partial t} \int_{cv} (u + \frac{v^2}{2}) \rho dv = - \int_{cs} (u + pv + \frac{v^2}{2}) \rho u dA\tag{A8}$$

Using the definitions of total temperature and specific heats and solving the integral for the lumped volume and the surface integral for the two ports yields:

$$\frac{\partial}{\partial t} (c_v \rho T) = \left[ (h + \frac{v^2}{2}) w \right]_2^1\tag{A8}$$

Substituting for  $\rho T = P/R$  and using the specific heat at constant pressure results in equation (5):

$$\frac{c_v}{R} \frac{d}{dt} (P) = [c_p T_1 w_1 - c_p T_2 w_2]\tag{A8}$$

$$\frac{d}{dt} (P) = \gamma R [T_1 w_1 - T_2 w_2]$$

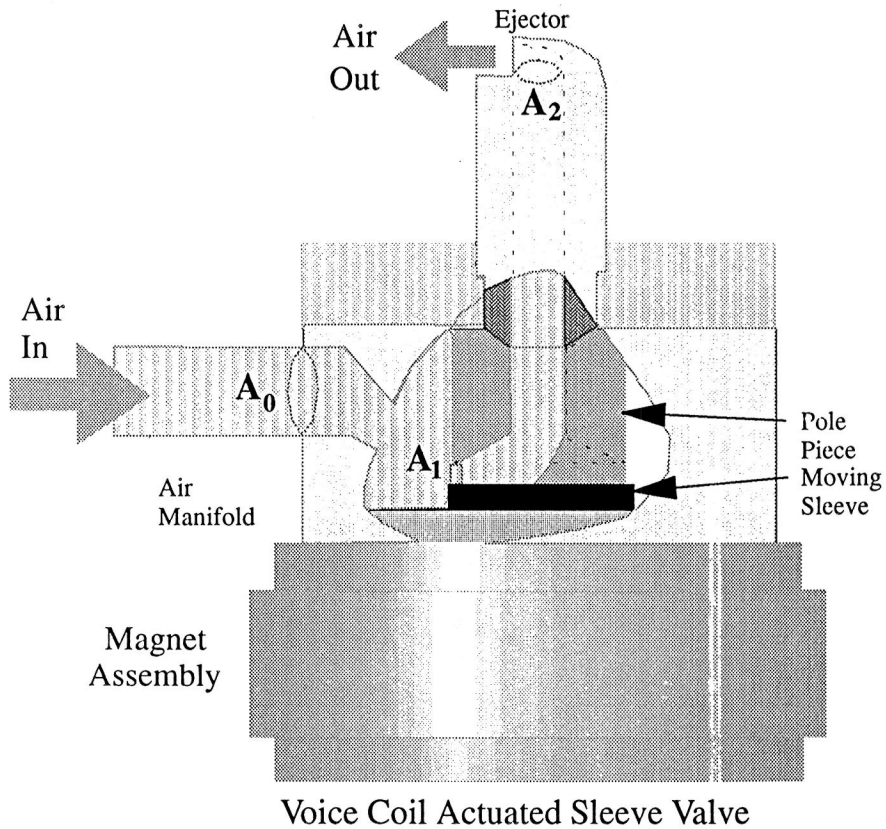
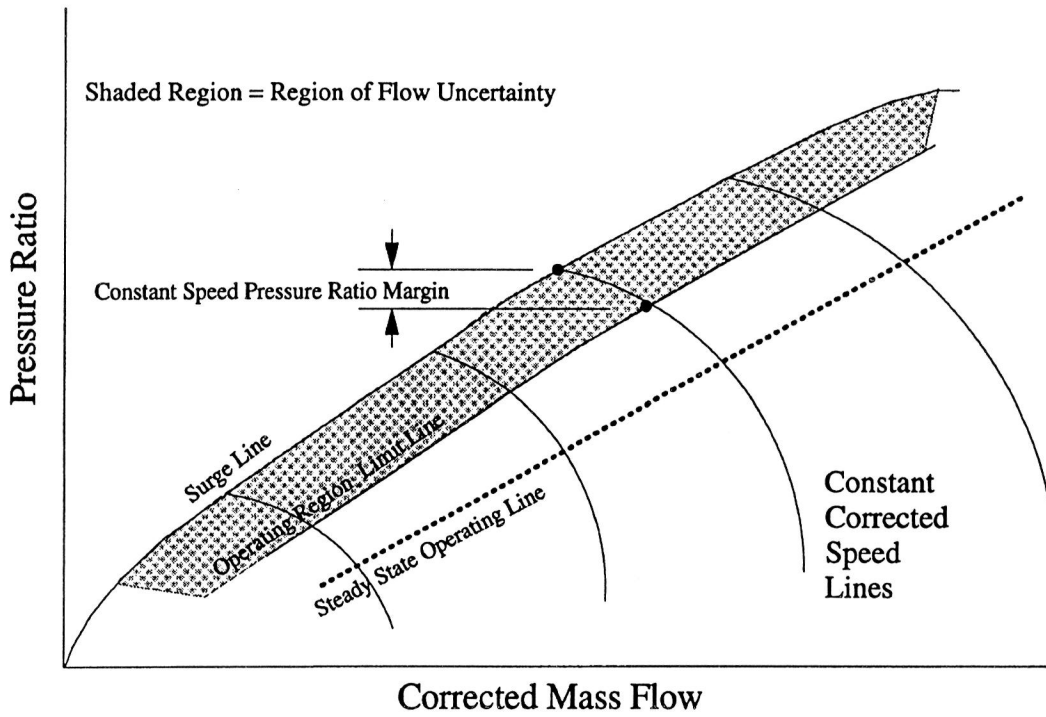


Figure 2 Prototype Valve Schematic

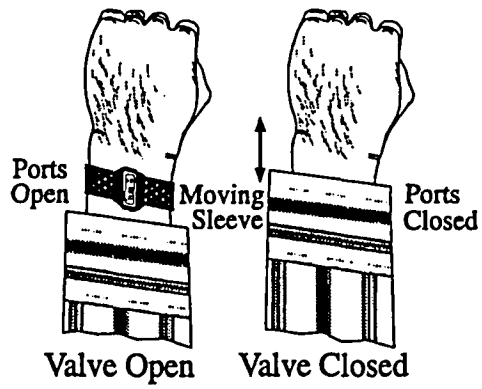


Figure 3 Description of a "Sleeve" Valve

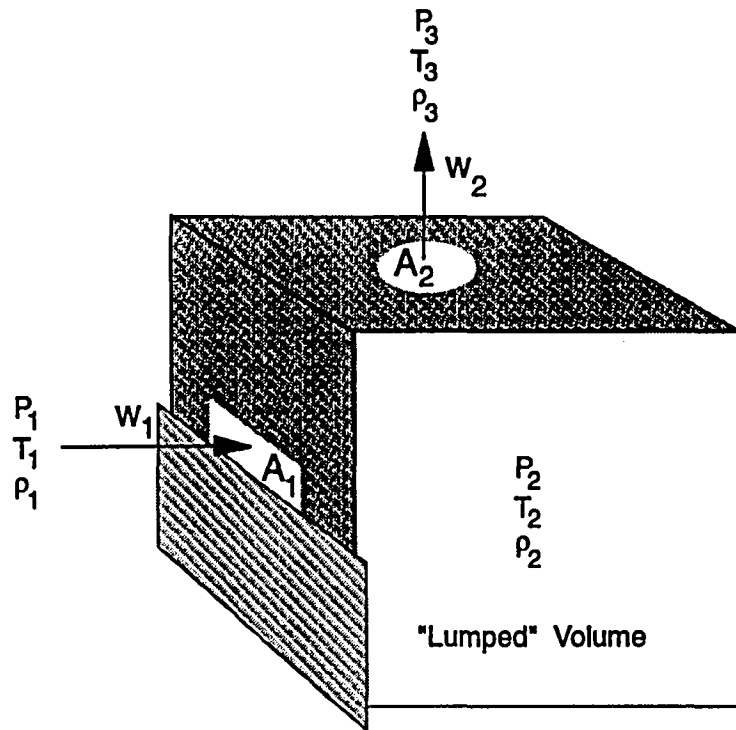


Figure 4 Schematic of Valve Model Geometry

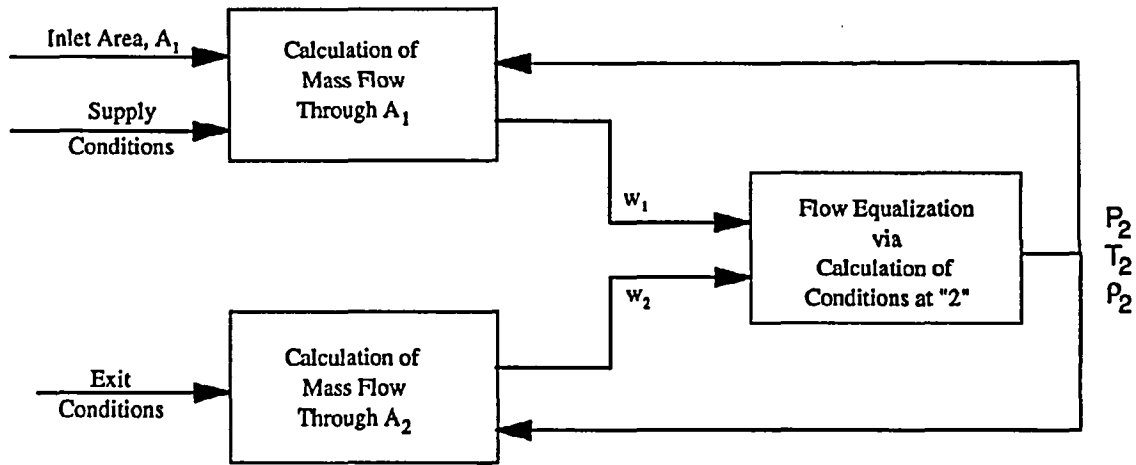


Figure 5 Math Model Block Diagram

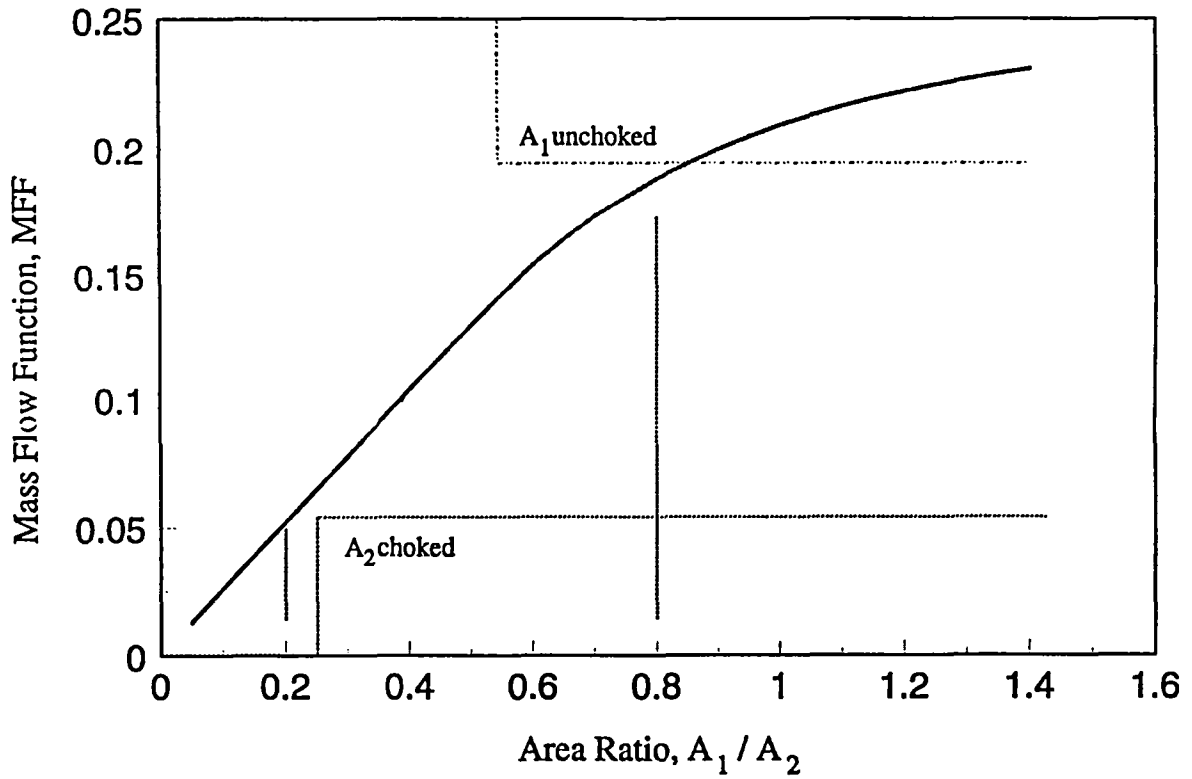


Figure 6 Nondimensional Mass Flow Function versus Area Ratio

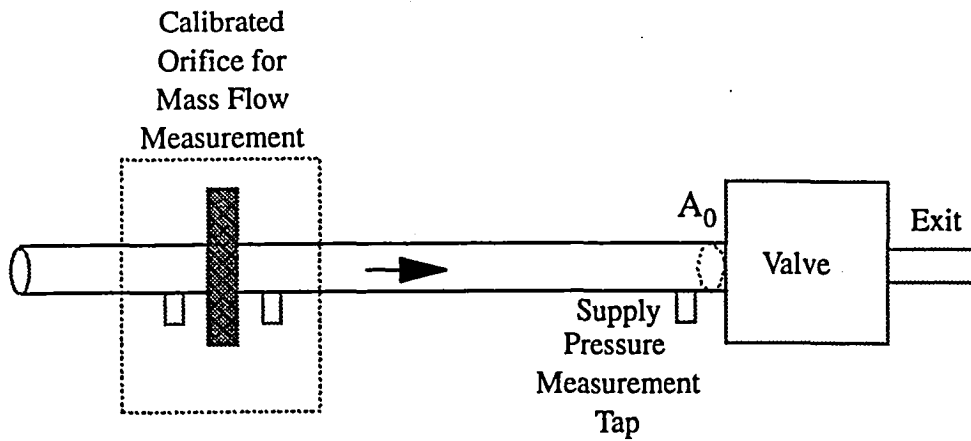


Figure 7 Schematic of Static Flow Calibration Setup

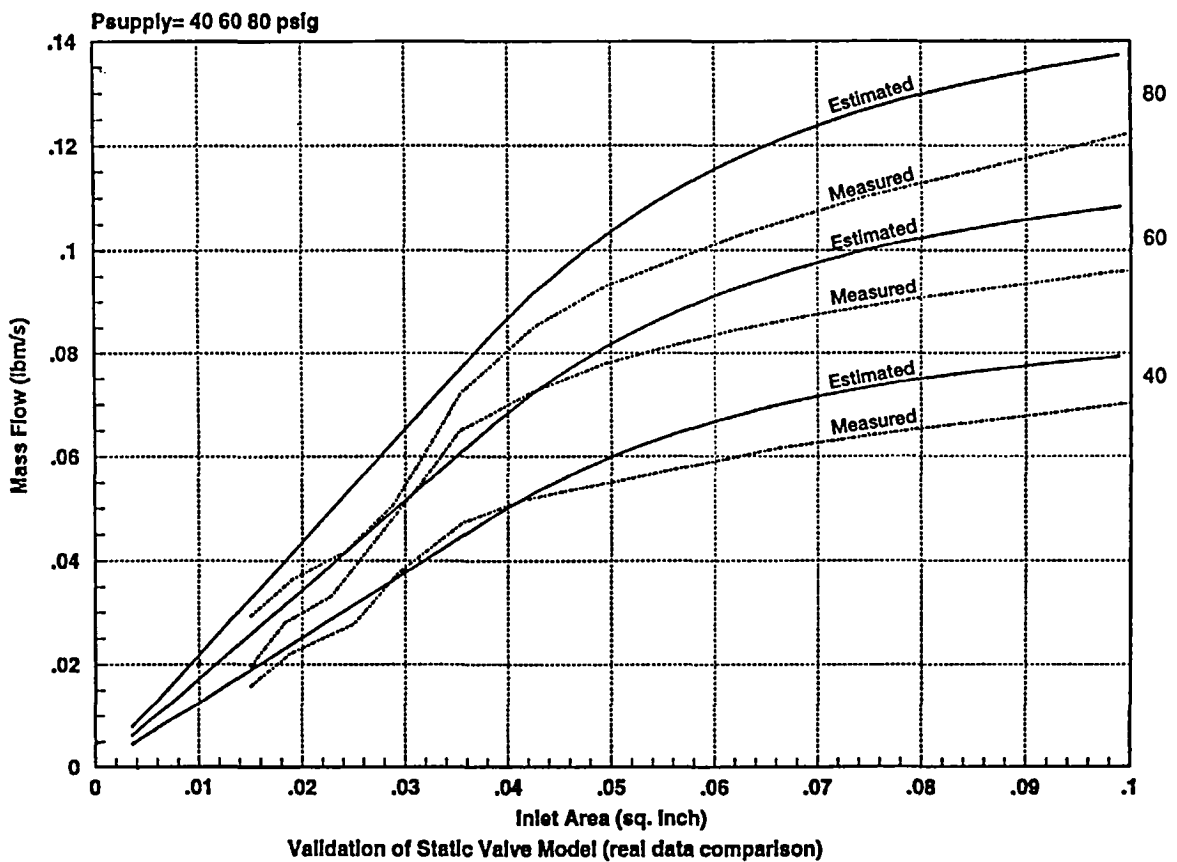


Figure 8 Comparison of the Model Predicted Mass Flow Rate to Experimental Data for 3 Supply Pressures

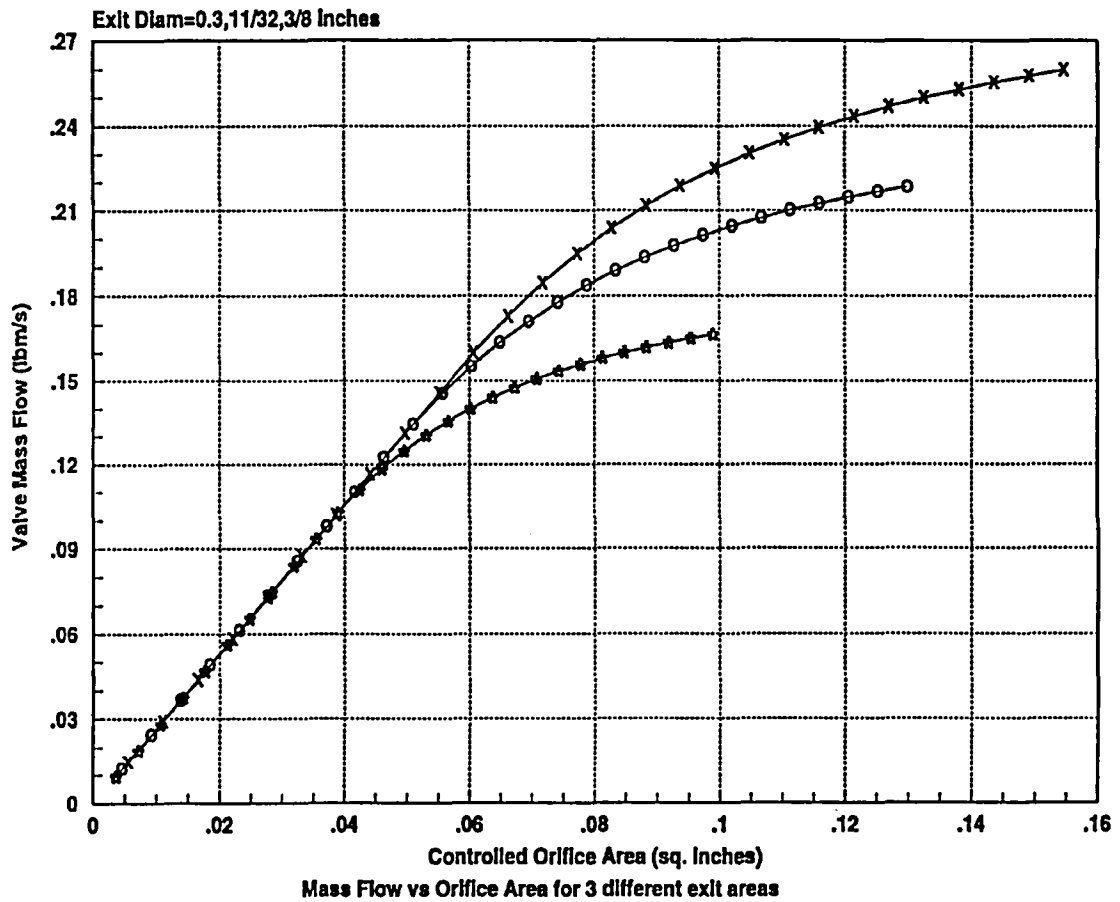


Figure 9 Comparison of the Mass Flow Rate versus Orifice Area for Three Different Exit Areas

# REPORT DOCUMENTATION PAGE

Form Approved  
OMB No. 0704-0188

Public reporting burden for this collection of information is estimated to average 1 hour per response, including the time for reviewing instructions, searching existing data sources, gathering and maintaining the data needed, and completing and reviewing the collection of information. Send comments regarding this burden estimate or any other aspect of this collection of information, including suggestions for reducing this burden, to Washington Headquarters Services, Directorate for Information Operations and Reports, 1215 Jefferson Davis Highway, Suite 1204, Arlington, VA 22202-4302, and to the Office of Management and Budget, Paperwork Reduction Project (0704-0188), Washington, DC 20503.

1. AGENCY USE ONLY (Leave blank)	2. REPORT DATE November 1995	3. REPORT TYPE AND DATES COVERED Technical Memorandum	
4. TITLE AND SUBTITLE  Static Flow Characteristics of a Mass Flow Injecting Valve		5. FUNDING NUMBERS  WU-505-62-50	
6. AUTHOR(S)  Duane Mattern and Dan Paxson		8. PERFORMING ORGANIZATION REPORT NUMBER  E-9936	
7. PERFORMING ORGANIZATION NAME(S) AND ADDRESS(ES)  National Aeronautics and Space Administration Lewis Research Center Cleveland, Ohio 44135-3191		10. SPONSORING/MONITORING AGENCY REPORT NUMBER  NASA TM-107072	
9. SPONSORING/MONITORING AGENCY NAME(S) AND ADDRESS(ES)  National Aeronautics and Space Administration Washington, D.C. 20546-0001		11. SUPPLEMENTARY NOTES Duane Mattern, NYMA Inc., 2001 Aerospace Parkway, Brook Park, Ohio 44142 (work funded by NASA Contract NAS3-25266) and Dan Paxson, NASA Lewis Research Center. Responsible person, Dan Paxson, organization code 2560, (216) 433-8334.	
12a. DISTRIBUTION/AVAILABILITY STATEMENT  Unclassified - Unlimited Subject Category 07  This publication is available from the NASA Center for Aerospace Information, (301) 621-0390.		12b. DISTRIBUTION CODE	
13. ABSTRACT (Maximum 200 words)  A sleeve valve is under development for ground-based forced response testing of air compression systems. This valve will be used to inject air and to impart momentum to the flow inside the first stage of a multi-stage compressor. The valve was designed to deliver a maximum mass flow of 0.22 lbm/s (0.1 kg/s) with a maximum valve throat area of 0.12 in <sup>2</sup> (80 mm <sup>2</sup> ), a 100 psid (689 KPA) pressure difference across the valve and a 68°F, (20°C) air supply. It was assumed that the valve mass flow rate would be proportional to the valve orifice area. A static flow calibration revealed a nonlinear valve orifice area to mass flow relationship which limits the maximum flow rate that the valve can deliver. This nonlinearity was found to be caused by multiple choking points in the flow path. A simple model was used to explain this nonlinearity and the model was compared to the static flow calibration data. Only steady flow data is presented here. In this report, the static flow characteristics of a proportionally controlled sleeve valve are modelled and validated against experimental data.			
14. SUBJECT TERMS  Static flow; Valve		15. NUMBER OF PAGES 16	
		16. PRICE CODE A03	
17. SECURITY CLASSIFICATION OF REPORT Unclassified	18. SECURITY CLASSIFICATION OF THIS PAGE Unclassified	19. SECURITY CLASSIFICATION OF ABSTRACT Unclassified	20. LIMITATION OF ABSTRACT